JOURNAL OF MATERIALS SCIENCE: MATERIALS IN MEDICINE **10** (1999) 841–846

A combined finite element method and continuum damage mechanics approach to simulate the *in vitro* fatigue behavior of human cortical bone

M. TAYLOR
Department of Orthopaedics, University Hospital in Lund, S-22185 Lund, Sweden and Mechanical Engineering Department, University of Southampton, Highfield, Southampton, SO17 1BJ, UK
E-mail: mtaylor@soton.ac.uk

N. VERDONSCHOT, R. HUISKES
Orthopaedic Research Laboratory, Department of Orthopaedics, University of Nijmegen, P.O. Box 9101, 6500 HB Nijmegen, The Netherlands

P. ZIOUPOS
Department of Materials and Medical Sciences, Cranfield University, Shrivenham SN6 8LA, UK

The fatigue of bone, in particular the associated modulus degradation and accumulation of permanent strain, has been implicated as the cause of femoral neck fractures and the migration of total joint replacements. The objective of this study was to develop a technique to simulate the tensile fatigue behavior of human cortical bone. A combined continuum damage mechanics (CDM) and finite element analysis (FEA) approach was used to predict the number of cycles to failure, modulus degradation and accumulation of permanent strain of human cortical bone specimens. The simulation of fatigue testing of eight dumb-bell specimens of cortical bone were performed and the predictions compared with existing experimental data. The predictions from the finite element models were in close agreement with the experimental data. The models predicted similar development of modulus degradation and permanent strain as observed in the experimental tests. The technique is capable of predicting the accumulation of permanent strain without the need for simulating every single load step. These findings suggest that the complex fatigue behavior of human cortical bone can be simulated using the described approach and forms the first step for simulating the more complex mechanisms associated with femoral neck fractures and implant migration.

1. Introduction

A number of experimental studies have investigated the fatigue behavior of human cortical bone. When subjected to long-term dynamic loading, cortical bone exhibits complex material behavior including a gradual reduction of elastic modulus, accumulation of permanent strain and failure at stress levels well below its static strength [1–3]. The degree of modulus degradation and accumulation of permanent strain appear to be dependent on the magnitude and sign of the applied stress/strain. Only a few authors have attempted to predict the fatigue behavior of bone using analytical techniques. Pattin *et al*. [2] presented an analytical expression, which adequately described the modulus degradation of human cortical bone subjected to tensile and compressive fatigue at a variety of stress levels. Griffin *et al*. [4] developed an analytical model to simulate the fatigue of cortical bone subjected to four-point bending. This model was based on beam theory for a composite material in which the osteons and interstitial cement were developing damage at different rates. The predictions for modulus degradation were in close agreement with experimental data from both uniaxial and four-point bend fatigue tests. Despite achieving reasonable correlations with the experimental data, both techniques only predict modulus degradation for specific geometries and loading configurations. To date, no attempt has been made to simulate the accumulation of permanent strain in cortical bone or to develop a technique applicable to any load case and any specimen geometry. The purpose of this study was to develop such a technique, with the ultimate aim being the application of similar techniques to simulate the failure processes associated with femoral neck fractures and migration of total joint replacements.

2. Materials and methods

Continuum damage mechanics (CDM) was implemented in conjunction with a finite element analysis (FEA) model to simulate the progressive accumulation of mechanical damage within a cortical bone specimen until gross failure of the sample occurred. A phenomenological damage parameter, ω, was used to represent the state of integrity of each finite element within the model at any given point in time during the simulation. Damage was assumed to be: (i) a linear function of the life fraction n/N_f, where n is the number of loading cycles and N_f is the number of loading cycles to failure [5]; (ii) zero at the beginning of the analysis rising to a value of 1 at failure; (iii) independent of the applied stress.

The number of loading cycles to failure, N_f, at a given stress level was determined from experimental fatigue data [3]

$$Log\,(N) = -28.23\,\log\,(\sigma/E_0) - 58.43 \quad (r^2 = 0.95) \tag{1}$$

where E_0 is the initial Young's modulus of the specimen and σ is the applied tensile stress. Both modulus and the accumulation of permanent strain were assumed to be non-linear functions of damage and expressions were derived, as a function of damage, from experimental fatigue data of eight dumb-bell specimens machined from the mid-diaphysis of a 27-year-old female [3]. For each individual specimen, the permanent strain data (unpublished) and variation in modulus data were fitted using equations of the form

$$E_n = a(\omega)^3 + b(\omega)^2 + c(\omega) + E_0 \tag{2}$$

$$\varepsilon_{pn} = d(\omega)^e \tag{3}$$

where E_n is the modulus after n loading cycles, ε_{pn} is the permanent strain after n loading cycles and a, b, c, d and e are material dependent constants. For all eight specimens the curve fit of the test data using Equations 2 and 3 was always better than $r^2 = 0.97$, with the exception of the modulus degradation data for one sample which had a correlation coefficient of 0.91. The results of linear regression analysis of the materials constants a to e derived from the eight specimens as a function of the effective strain were

$$a = 2.346(\sigma/E_0) - 19032 \quad (r^2 = 0.80) \tag{4}$$

$$b = -2.567(\sigma/E_0) + 21737 \quad (r^2 = 0.69) \tag{5}$$

$$c = -1.425(\sigma/E_0) + 4302 \quad (r^2 = 0.58) \tag{6}$$

$$d = 0.931(\sigma/E_0) - 3395 \quad (r^2 = 0.76) \tag{7}$$

$$e = 1.52 \times 10^{-4}(\sigma/E_0) - 0.525 \quad (r^2 = 0.70) \tag{8}$$

It should be noted that two samples were discounted from the regression analysis of material constants d and e as they produced significantly different permanent strain plots as compared to the other samples. Combining Equations 2, 4, 5 and 6 formed a generalized equation for the variation of modulus as a function of damage. Combining Equations 3, 7 and 8 developed a generalized equation for the accumulation of permanent strain. These generalized equations were used for all subsequent finite element simulations.

An iterative solution procedure was adopted. The simulation of every loading cycle would have been computationally expensive. Therefore, each simulation consisted of a number of iterations, and depending on the magnitude of the applied stress, each iteration represented the action of ten to tens of thousands of load cycles. At the beginning of each iteration, the finite element model was loaded and the stresses within each element calculated. From Equation 1, the number of loading cycles to failure, N_f, within each element was calculated, and the element with the lowest number of cycles to failure within the finite element mesh determined. The increment in the number of loading cycles, Δn, was calculated based on a predetermined percentage of the lowest number of loading cycles to failure. The increment in damage, $\Delta\omega$, within each finite element was calculated and added to the total damage, ω, accumulated so far. If damage reached a value of 1, the relevant element was removed from the analysis and the load redistributed to the surrounding elements.

The increase in strain due to modulus degradation and the accumulation of permanent strain was calculated based on Equations 2 and 3 and the materials constants derived in Equations 4 to 8. As the material constants were dependent on the effective strain, each constant had to be calculated on an element by element basis. The constants were calculated within the first iteration, stored and used through out the remainder of the analysis. The additional strain was added to the model as creep at the end of each iteration, using the user subroutine UCREEP within the Marc finite element solver. At the beginning of the next iteration, the stiffness matrix was updated and the stresses recalculated. The whole procedure was then repeated a number of times, until failure of the sample occurred.

The technique was tested by simulating the tensile fatigue tests of Zioupos *et al.* [3]. A three-dimensional finite element model of a dumb-bell specimen of human cortical bone was generated, as described by Zioupos *et al.* [3]. Only one quarter of the specimen was modelled (Fig. 1) due to symmetry and the appropriate symmetry constraints were applied. The model consisted of 599 eight-noded reduced integration elements and 910 nodes. The cortical bone was assumed to be isotropic, homogeneous and linear elastic, with a Poisson's ratio of 0.35. No attempt was made to simulate the cyclic visco-elastic properties of cortical bone. All analyses were performed using Marc version 7.3.

Simulations of the fatigue testing of eight cortical bone samples were performed at a variety of stress levels. A summary of the specimen data is given in Table I. In each case, the only data supplied to the finite element model was the initial Youngs' modulus and the magnitude of the applied load. The simulations were run until the specimen was deemed to have failed, i.e. when a band of elements through the cross-section of the specimen had reached a damage value of 1. In each case, the number of loading cycles to failure, modulus degradation and accumulated permanent strain were calculated and the results compared with the experimental data.

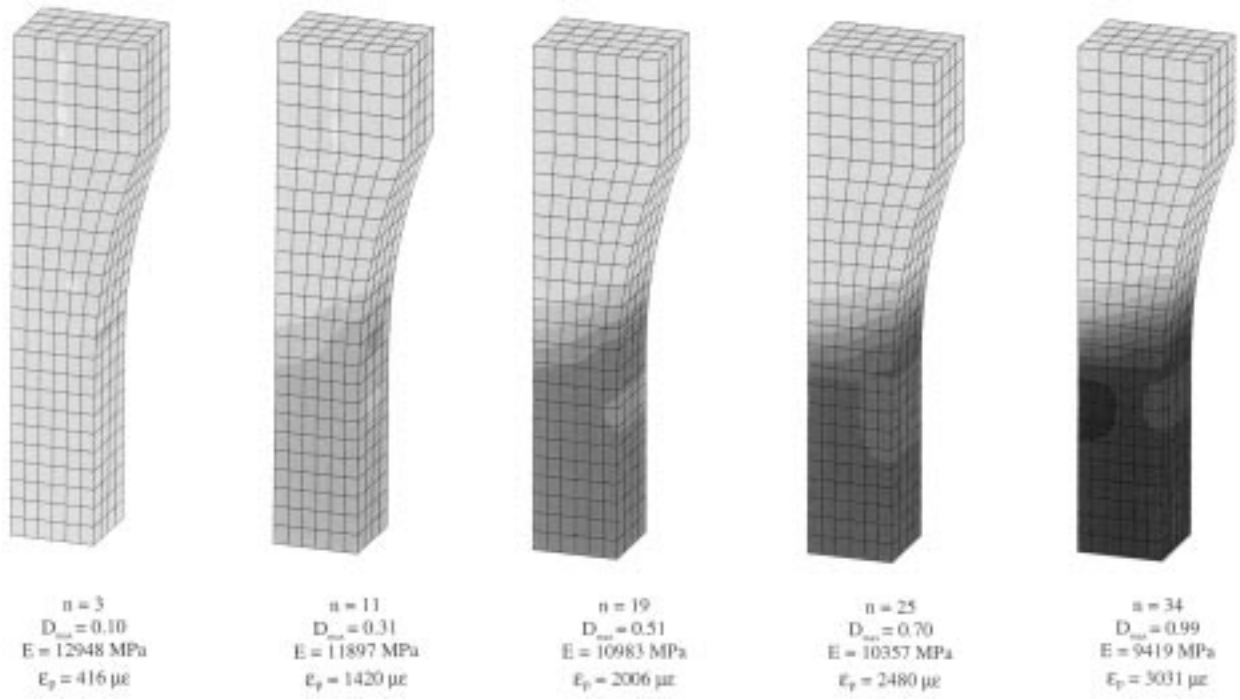

Figure 1 The formation and progression of damage during the simulation of the fatigue test performed on sample 1 (n = number of loading cycles, D_{max} = maximum damage present in the specimen, E = current modulus at the center of the specimen, ε_p = current permenant strain at the center of the specimen). Light gray corresponds to no damage ($\omega = 0$), black to complete failure ($\omega = 1$).

3. Results

Fig. 1 illustrates the accumulation of damage during the simulation of the fatigue testing of sample 1. The initial damage pattern is not as uniform as would be expected for a dumb-bell specimen. In the early stages of fatigue the highest areas of damage occur around the shoulder of the specimen. However, the resultant reduction in modulus transfers the load into the gauge length of the specimen. This region then gradually accumulates damage until gross failure occurs.

Comparison of the predicted modulus degradation and permanent strain data with the experimental results are shown in Figs 2 and 3, respectively. In general, the results of the finite element simulations were in close agreement with the experimental data, both in terms of the trends and absolute magnitudes. The samples subjected to low effective strain, high cycle fatigue exhibited minimal modulus degradation or accumulation of permanent strain until near the end of their fatigue life. For these samples (specimens 5, 7 and 10) the predicted modulus degradation and permanent strains were in close agreement with the experimental data for approximately 95% of their fatigue life, but the models were unable to predict the rapid loss of modulus and rapid accumulation of strain which occurred in the last 5% of the test. The samples subjected to high initial strain, low cycle fatigue showed continuous modulus degradation and permanent strain accumulation throughout the test. In these cases the finite element models were able to predict the modulus degradation and the permanent strains throughout the fatigue test. With the exception of sample 9, at a life fraction (n/N) of 0.9 the predicted moduli were within 5% of the experimental values. For sample 9, the predicted modulus at a life fraction of 0.9 was 22% higher than the experimentally measured value. The predicted permanent strains were within 15% of the experimental values for six out of eight of the specimens at a life fraction of 0.9. The exceptions were samples 9 and 10. In both cases the finite element models severely underestimated the permanent strains. Examination of the experimental data reveals that these samples do not behave in the same manner as the other specimens, developing far more permanent strain than would have been expected at their respective effective strain levels.

TABLE I Experimental data for the eight cortical bone samples subjected to tensile fatigue

Sample ID	Initial modulus (MPa)	Applied stress (MPa)	Initial strain (microstrain)
1	13100	94.0	7175
2	15600	122.0	7820
3	17300	114.0	6589
5	14900	83.0	5570
7	15000	86.0	5733
8	15400	110.0	7142
9	15100	104.0	6887
10	16700	100.0	5998

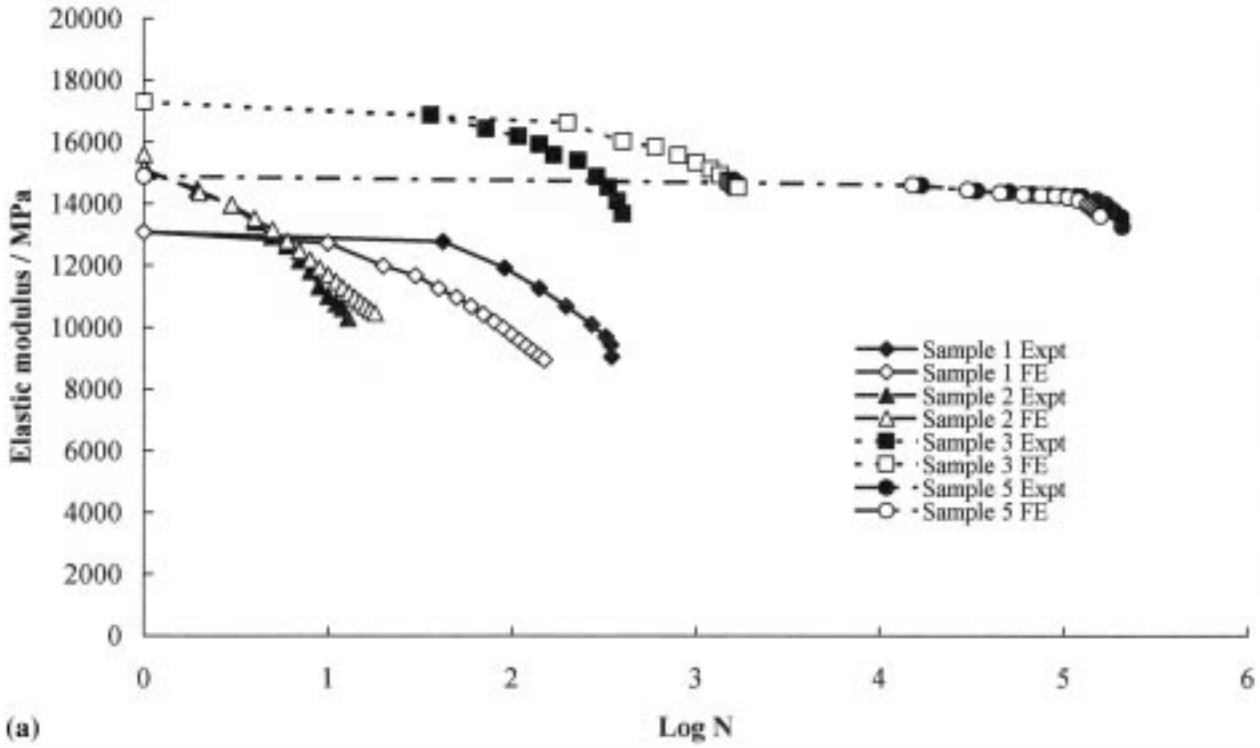

(a)

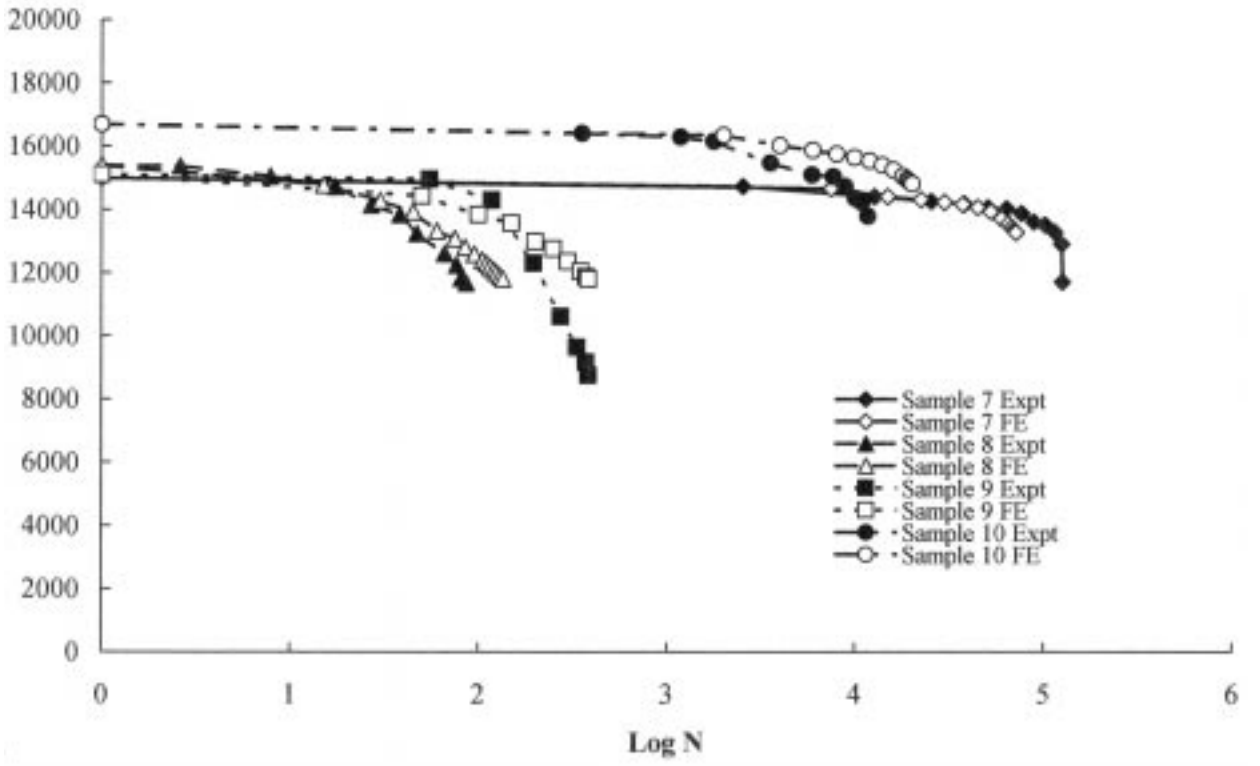

(b)

Figure 2 Comparison of the measured and predicted modulus degradation for (a) samples 1, 2, 3 and 5 and (b) samples 7, 8, 9 and 10.

4. Discussion

The objective of this study was to develop a combined continuum damage mechanics and finite element approach to simulate the fatigue behavior of human cortical bone. Others have attempted to predict the number of loading cycles to failure and modulus degradation [2, 4]. However, this is the first time that a model has also been able to predict the development of permanent strain. By coupling both the elastic modulus and permanent deformation to damage, realistic stress–strain histories in uniaxial tension can be simulated.

The main advantage of this technique is that it allows the simulation of the fatigue process without having to simulate every load step, dramatically reducing the computational cost. Additionally, the technique is not restricted to specific geometries and loading conditions. The main limitation of the study is that damage was assumed to be a scalar quantity, which is a reasonable

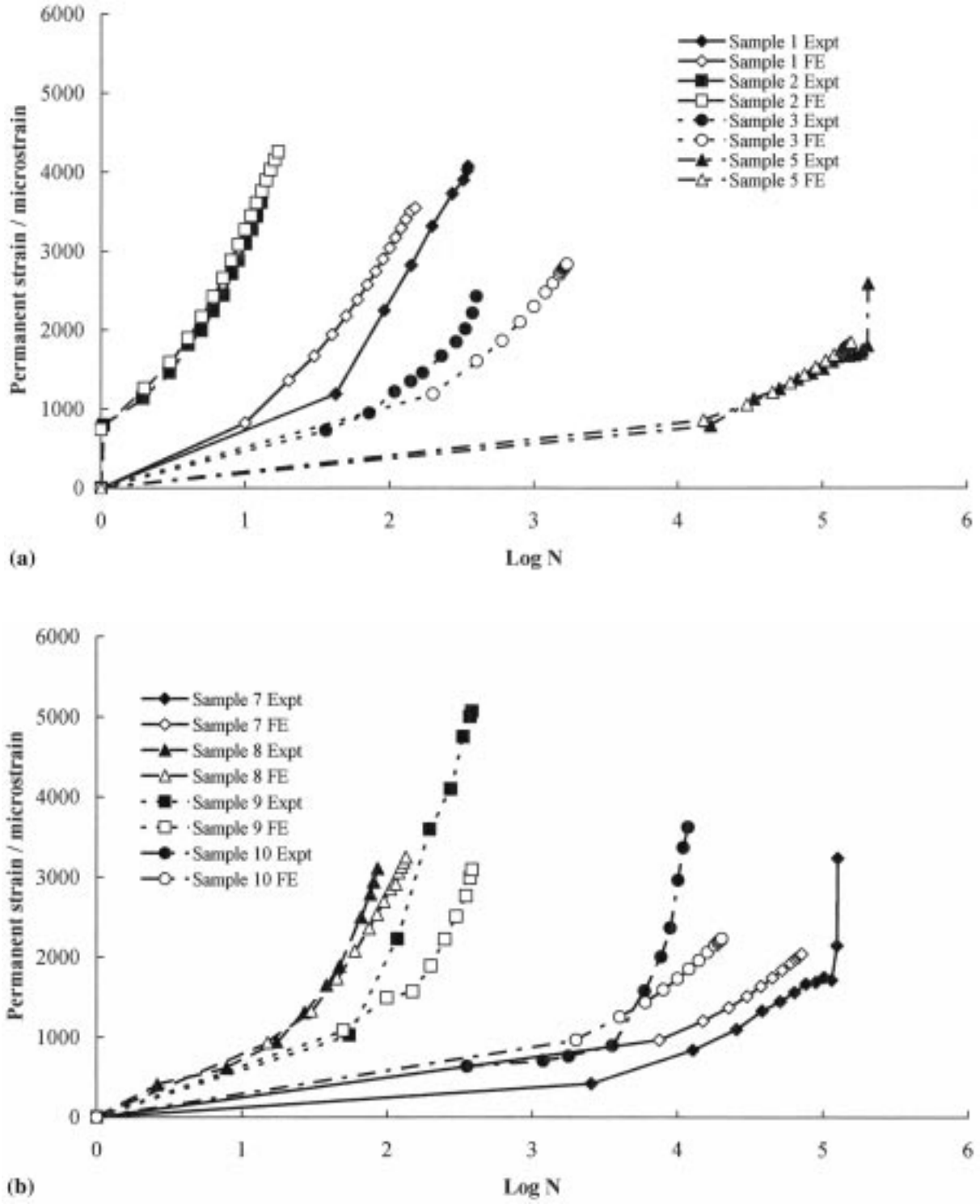

Figure 3 Comparison of the measured and predicted development of permanent strain for (a) samples 1, 2, 3 and 5 and (b) samples 7, 8, 9 and 10.

assumption for uniaxial loading. However, for more complex problems, damage would have to be modeled as a vector quantity.

There has been little debate, if any, as to the role of permanent strain *in vivo*. It seems unlikely that in healthy cortical bone there is any significant development of permanent deformations during normal activities. However, modulus degradation and the formation of permanent strains may contribute to the development of stress fractures and degenerative diseases like osteoarthritis. The development of permanent strain is particularly relevant to cancellous bone, as can be seen in the progressive collapse of spinal vertebra and may also play an important role in the migration and aseptic loosening of total joint replacements [6]. Radiographic studies have shown that migration, the progressive displacement of the implant relative to the bone, can be used to predict the incidence of loosening [7, 8]. Linder [9] stated that migration can only occur as a result of remodeling or impaction of the bone immediately surrounding the implant. The ability to simulate the formation of permanent strain may, therefore, be the first step in developing a preclinical test to predict the likelihood of implant migration.

Acknowledgments

Dr Taylor would like to thank Action Research and the Royal Academy of Engineering for funding this research.

References

1. D. R. CARTER and W. E. CALER, *J. Biomech.* **14** (1981) 461.
2. C. A. PATTIN, W. E. CALER and D. R. CARTER, *ibid.* **29** (1996) 69.
3. P. ZIOUPOS, X. T. WANG and J. D. CURREY, *Clin. Biomech.* **11** (1996) 365.
4. L. V. GRIFFIN, J. C. GIBELING, R. B. MARTIN, V. A. GIBSON and S. M. STOVER, *J. Orthop. Res.* **15** (1997) 607.
5. M. A. MINER, *J. Appl. Mech.* (1945) 159.
6. M. TAYLOR and K. E. TANNER, *J. Bone Joint Surg.* **79B** (1997) 181.
7. L. RYD, B. E. J. ALBREKTSSON, L. V. CARLSSON, F. DANSGARD, P. HERBERTS, A. LINDSTRAND, L. REGNER and S. TOKSVIG-LARSEN, *ibid.* **77B** (1995) 377.
8. M. A. R. FREEMAN and P. PLANTE-BORDENEUVE, *ibid.* **76B** (1994) 432.
9. L. LINDER, *Acta Orthop. Scand.* **65** (1994) 654.

Received 10 May
and accepted 2 June 1999